Admittance based Adaptive Cooperative Control for Multiple Manipulators with Output Constraints

Yong Li, Chenguang Yang, Weisheng Yan, Rongxin Cui, Andy Annamalai

***Abstract*—This paper proposes a novel adaptive control methodology based on admittance model for multiple manipulators transporting a rigid object cooperatively along a predefined desired trajectory. Firstly, an admittance model is creatively applied to generate reference trajectory online for each manipulator according to the desired path of the rigid object, which is the reference input of the controller. Then, an innovative integral Barrier Lyapunov function (iBLF) is utilized to tackle the constraints due to the physical and environmental limits. Adaptive neural networks (NN) are also employed to approximate the uncertainties of the manipulator dynamics. Different from the conventional NN approximation method, which is usually semi-globally uniformly ultimately bounded (SGUUB), a switching function is presented to guarantee the global stability of the closed-loop. Finally, the simulation studies are conducted on planar 2-link robot manipulators to validate the efficacy of the proposed approach.**

***Index Terms*—Neural networks; Robot manipulators; Admittance control; Barrier Lyapunov function (BLF); Globally uniformly ultimately bounded (GUUB)**

I. Introduction

In recent decades, robots have been widely employed in a variety of applications, such as entertainment, manufacturing industry and medical service [1], [2], etc. Among these applications, robot manipulators play a significant role and hence has attracted a lot of attention. Subsequently, large amount of efforts have been dedicated to the advance of robot manipulator technology [3]–[8]. An increasing complexity of tasks performed by robots demand higher manipulation skills and has rendered single manipulators ineffective in many situations. Hence, the research about coordinated multiple manipulators is becoming progressively significant [9]–[11]. For instance, the problem of transporting a long, heavy object has been studied in [12], where the task was accomplished easily with the cooperation of multiple robots.

This work was supported in part by National Natural Science Foundation of China under Grants 61733014, 61472325, 51579210 and 61633002, and Engineering and Physical Sciences Research Council (EPSRC) under Grant EP/S001913/1. (Corresponding authors are Chenguang Yang and Rongxin Cui).

Y. Li, W. Yan and R. Cui are with the School of Marine science and Technology, Northwestern Polytechnical University, Xi'an 710072, China (e-mail: 917746@swansea.ac.uk, r.cui@nwpu.edu.cn, wsyan@nwpu.edu.cn).

C. Yang is with Bristol Robotics Laboratory, University of the West of England, Bristol, BS16 1QY, U.K. (e-mail: cyang@ieee.org).

Andy Annamalai is with University of Winchester, U.K. (email: Andy.Annamalai@winchester.ac.uk).

The manuscript is submitted to the TNNLS special issue on Intelligent Control through Neural Learning and Optimization for Human Machine Hybrid Systems.

However, the cooperative control of multi-manipulators is much more complicated than that of single one. The complex dynamics due to the presence of a large number of degrees of freedom (DOFs) of multiple manipulators in a system, result in a closed holonomic constrained chain mechanism [13]. In [14], a compound position/force control strategy was investigated under the assumption that an object was carried without relative motion between the object and manipulators. However, the relative motion between manipulators during the cooperative movement exists for a number of applications. A self-tuning control for cooperative manipulators was studied in [15], where the closed kinematic chain was formed by manipulators in the presence of uncertainty of kinematics model. Two cascaded estimators were adopted to change the kinematic parameters online to attain a good tracking performance. A flexible payload transforming problem for multiple collaborative agents was addressed in [16], which was regarded as a formation control problem by modelling the contact forces as the gradients of nonlinear potentials.

For multiple manipulators transporting a rigid object, some properties of grasp need to be taken into consideration. In grasp planning, there are two main classes of grasps known as "form closure" and "force closure" grasps [17]. These terminologies were first used by Reuleaux [18] in 1875 when he investigated the mechanism of some machines. Form closure is a pure geometry property, which describes the capability that the contacts can prevent all motions of a grasped object [17]. Reuleaux found that to obtain the form closure property, at least four contact points are needed in a planar case and Somov reported the number for a general spatial case is at least seven [19]. A further detailed classification of form closure can be seen in [20]. The significant difference between force-closure and form-closure is whether the friction forces are considered or not [21]. The manner in which the contact forces are being exerted on the object and the kinematics of the manipulators are contained by Force closure.

Investigations of interaction control mainly include force control and impedance control. Impedance control was introduced in [22], with the kernel idea of taking the mechanical impedance into consideration and mapping from state of the system to the interaction forces. The feasible, robust impedence control can be seen in [13], [23], [24]. On the contrary, another control method called admittance can be regarded as an inverse process of impedance control, mapping from forces to desired trajectory [25]. In conventional admittance control system, with predefined desired trajectory and the interaction forces exerted on the object, a virtual desired trajectory can be obtained. In this paper, an admittance model with interaction

force between manipulators and object (measured by pressure sensors) is utilized to generate reference trajectories online for each manipulator.

In practical applications, there are still considerable difficulties to determine the precise actual kinematic and dynamic models of robots due to the uncertainties and environmental disturbances. Therefore, neural networks based methods have been widely employed in designing adaptive controller in the absence of availability of a precise model of the system [26]–[32]. The radial basis function Neural Networks (RBFNN) is a highly effectively tool for obtaining a model due to its universal approximation ability, which means it can approximate a smooth nonlinear function, and hence has been extensively utilized in designing controller for uncertain or unknown system [6]. In [33], the NN approximation strategy was used to compensate for the uncertain dynamics of the manipulated object and the robot manipulator. A class of multi-input-multi-output (MIMO) nonlinear manipulators adaptive control problem was investigated in [34]. In this work, two RBFNN namely, a critic NN and an actor NN are employed to achive the optimal control. Control method based on adaptive RBFNN to guarantee the global stability was developed in [35]–[38]. To deal with the unknown system paramters and complex couplings among several subsystems, an ANN was presented in [39].

It is noted that the conventional NN approximation method can only guarantee the semi-globally uniformly ultimately bounded (SGUUB) stability of the closed-loop system, which means the NN approximator is only valid in its active domain. Therefore it is essential to design NN controller with globally uniformly ultimately bounded (GUUB) stability [40], [41]. In [41], a novel switching scheme was introduced by combining a robust controller with an adaptive neural controller in the approximation domain, to guaranteed that the states in closed-loop system are GUUB.

The actual control system always faces some limitations in practical situations, such as state constraints, input and output constraints, etc. Barrier Lyapunov Function (BLF) was proposed due to its advantage of achieving a good tracking performance and satisfying the constraints simultaneously [42]. By utilizing some barrier functions whose value is infinite at corresponding limits, these methodologies keep the barriers not to be violated. As a consequence, the constraints are guaranteed to be valid all the time. BLFs are used for designing controller in several forms, for instance, Brunovsky form [43], feedback output-constrained system [44], state-constrained system [45]. Compared with the generalized BLF whose constraints tend to be more conservative, an improved approach named integral barrier Lyapunov function (iBLF) [46] for nonlinear system allows the mixture of the initial state constraints and the errors. In this paper, iBLF is also presented in the analysis of system stability.

Inspired by the aforementioned discussion, a control scheme for a multiple homogeneous manipulators system grasping an object and tracking a predefined trajectory without knowing the precise system model is designed in this paper. For clarity, the main contributions of this paper are highlighted as follows:

1) The admittance model is introduced to work as a trajectory generator, which also depicts the interaction between the object and manipulators. Once the desired trajectory of the carried object is given, the reference trajectory for each manipulator could be generated online.
2) A novel iBLF function is presented in this paper. The iBLF function is of great significance in dealing state constraints.
3) An NN control scheme is proposed by combing a switch function with an adaptive neural network. Such a scheme could achieve a global approximation for the uncertainties in the system dynamics.

Then a global RBFNN based adaptive control approach is specially designed for each manipulator to track the corresponding reference trajectories. By learning from system states and applying updating law for the weight matrix, optimal estimated weight matrix of the neural networks is obtained.

The structure of this paper is organised as follows. Section II formulates the problem and introduces some preliminaries. In section III, the multiple manipulators model is presented and the trajectory generator is designed. Section IV proposes the control strategy and the proof of system stability. In Section V, the simulation studies are conducted to verify the proposed methodology. The conclusion is drawn in Section VI.

II. Problem Formulation and Preliminaries

A. Problem Formulation

Consider a system with multiple homogeneous robot manipulators, the coordinated task is for m manipulators to grasp and move an object along a predefined trajectory, as shown in Fig.1. The forces between the manipulators and the object can be measured by the pressure sensors. By employing admittance model [25] which mapping from forces to trajectories, the reference trajectories are obtained and tracked. In order to successfully fulfil the task, the following control objectives need to be accomplished:

(i) the reference trajectory can be generated by using admittance method.

(ii) the end-effectors of the manipulators could track the reference end-effectors trajectories and the actual trajectories should be bounded within a predefined range due to the practical limitation.

(iii) the contact force between the object and manipulators could be restricted within an allowable range, in case of damaging to the object.

Before discussing the control of multiple manipulators, we need to take the contacts on the rigid object into consideration. Therefore, the following assumption is considered as a premise of the proposed method.

Assumption 1: The holding of the rigid object by multiple manipulators is form-closured, which means the contacts between manipulators and object prevent all kinds of motions of the rigid object.

Assumption 2: The end-effector is rigidly attached to the object, i.e., there is no relative movement between the end-effector and the object.

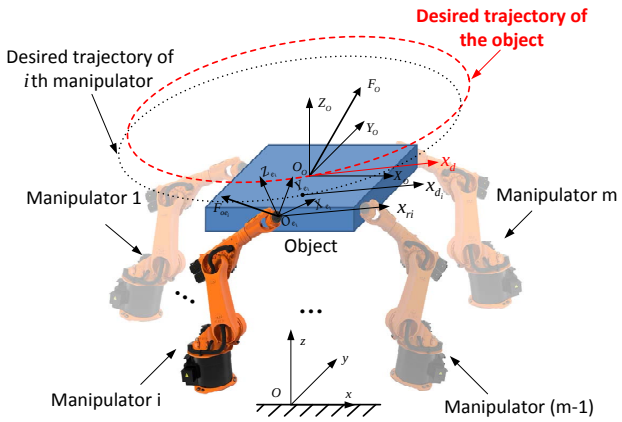

Fig. 1. A typical illustration of multiple robot manipulators carrying an object

B. Robot Manipulator Dynamics

In this paper, a class of rigid robot manipulators with n-degree of freedom (DOF) has been considered. The dynamics of the ith manipulator [47] is represented as follows:

$$\begin{aligned} &M_{e,i}(q_i)\ddot{q}_i + C_{e,i}(q_i,\dot{q}_i)\dot{q}_i + G_{e,i}(q_i) \\ =&\tau_{e,i} + J_{e,i}^T(q_i)F_i \end{aligned} \tag{1}$$

where $q_i, \dot{q}_i, \ddot{q}_i \in \mathbb{R}^{N_i}$ are the joint position, joint velocity and joint acceleration, respectively, $M_{e,i}(q_i) \in \mathbb{R}^{N_i \times N_i}$ denotes the symmetric positive definite inertia matrix, $C_{e,i}(q_i,\dot{q}_i) \in \mathbb{R}^{N_i \times N_i}$ is the Coriolis-centrifugal torque matrix, $G_{e,i}(q_i) \in \mathbb{R}^{N_i}$ denotes the gravity torque vector; $\tau_{e,i} \in \mathbb{R}^{N_i}$ stands for the control input torque vector, F_i is the force vector exerted on the end-effector of the ith manipulator, $N_i (i = 1, \cdots, m)$ stands for the number of the ith manipulator's DOF, and m is the number of manipulators.

Considering the position of the end-effector of the ith manipulator $x_i \in \mathbb{R}^{n_i}$ in the Cartesian space, the kinematics of the ith manipulator is $x_i = \phi_i(q_i)$. Differentiate the kinematics with regards to time yields

$$\dot{x}_i = J_{e,i}(q_i)\dot{q}_i \tag{2}$$

where $J_{e,i}(q_i) \in \mathbb{R}^{n_i \times N_i}$ is the Jacobian matrix. The dynamics of ith manipulator in Cartesian space can be represented as below

$$\begin{aligned} &M_i(q_i)\ddot{x}_i + C_i(q_i,\dot{q}_i)\dot{x}_i + G_i(q_i) \\ =&\tau_i + F_i \end{aligned} \tag{3}$$

where

$$\begin{aligned} M_i(q_i) =& J_{e,i}^{-T}(q_i)M_{e,i}(q_i)J_{e,i}^{-1}(q_i) \\ C_i(q_i,\dot{q}_i) =& J_{e,i}^{-T}(q_i)\big(C_{e,i}(q_i,\dot{q}_i) - M_{e,i}(q_i) \\ & J_{e,i}^{-T}(q_i)\dot{J}_{e,i}(q_i)\big)J_{e,i}^{-1}(q_i) \\ G_i(q_i) =& J_{e,i}^{-T}(q_i)G_{e,i}(q_i) \\ \tau_i =& J_{e,i}^{-T}(q_i)\tau_{e,i} \end{aligned} \tag{4}$$

The rigid robot manipulators depicted in (1)have the following properties [47] :

Property 1: The skew-symmetric matrix $2C_i(q_i,\dot{q}_i) - \dot{M}_i(q_i) \in \mathbb{R}^{n_i \times n_i}$ satisfies that

$$x^T[\dot{M}_i(q_i) - 2C_i(q_i,\dot{q}_i)]x = 0, \forall x \in \mathbb{R}^{n_i} \tag{5}$$

Property 2: The symmetric and positive definite inertia matrix $M_i(q_i)$ is uniformly bounded, there exists lower limit constant $\underline{m}_i > 0$ and upper limit constant $\overline{m}_i > 0$, and $M_i(q_i)$ satisfies the following inequality

$$\underline{m}_i \leqslant ||M_i(q_i)|| \leqslant \overline{m}_i \tag{6}$$

Property 3: The matrix $C_i(q_i,\dot{q}_i)$ and the vector $G_i(q_i)$ are bounded by $||C_i(q_i,\dot{q}_i)|| \leqslant k_{c_i}||\dot{q}_i||$, and $||G_i(q_i)|| \leqslant k_{g_i}$, respectively, where k_{c_i} and k_{g_i} are positive constants.

C. RBFNN Constructure

According to the Weierstrass high order Approximation Theorem [48], given sufficient basis nodes, every continuous function $F(Z) : \Omega_z \to \mathbb{R}$ over a compact set $\Omega_Z \subset \mathbb{R}^{N_{in}}$ can be approximated as closely as desired by utilizing a basis set $\{s(z)\}$ [49]. In this paper, Gaussian radial basis function is applied to approximate nonlinear function. The RBFNN structure is represented as follows:

$$F(W,Z) = W^{*T}S(Z) + \varepsilon(Z), \quad \forall Z \in \Omega_Z \tag{7}$$

where $Z = [z_1, z_2, \cdots, z_{N_{in}}] \in \mathbb{R}^{N_{in}}$ is NN input vector, $W^* = [w_1^*, w_2^*, \cdots, w_{N_o}^*] \in \mathbb{R}^{N_s \times N_o}$ is an ideal constant weight vector, $S(Z) = [s_1(Z), s_2(Z), ..., s_{N_s}(Z)]^T$ is the regressor vector with Gaussian radial basis function $s_i(\cdot)$, $\varepsilon(Z) \in \Omega_z$ is the approximation error and $|\varepsilon(Z)| < \varepsilon^*$ with constant $\varepsilon^* > 0$ for all $Z \in \Omega_Z$, N_{in} and N_o are control input and output dimension, respectively, N_s is the number of neural nodes.

The Gaussian function is chosen as follows:

$$s_i(\|Z - \mu_i\|) = \exp\left[\frac{-(Z-\mu_i)^T(Z-\mu_i)}{\vartheta_i^2}\right] \tag{8}$$

where $\mu_i = [\mu_{i1}, \mu_{i2}, \cdots, \mu_{iN_{in}}]^T (i = 1, 2, \cdots, N_{in})$ is the center of the neuron node, and ϑ_i is the width of the Gaussian function.

It is noted that the ideal weight matrix W^* is usually unknown in (7). In practice, the estimated weight $\hat{W}$, which can be trained by a weight updating law, is often used to replace W^* to approximate an nonlinear function, thus RBFNN in (7) can be represented as:

$$\hat{F}(Z) = \hat{W}^T S(Z) \tag{9}$$

III. Modelling Procedure

A. Dynamics of Multiple Manipulators

The dynamics of the object is:

$$M_o(x_o)\ddot{x}_o + C_o(x_o,\dot{x}_o)\dot{x}_o + G_o(x_o) = F_o - F_d \tag{10}$$

where $F_o \in \mathbb{R}^n$ is the resulting force exerted on the object, F_d stands for the envirmonment force vector exerted on the object.

From Assumption 2, let $J_i(x_o) \in \mathbb{R}^{n_i \times n}$ be the Jacobian matrix relating the the position of the end-effector $x_i \in \mathbb{R}^{n_i}$

with the mass centre of the object $x_o \in \mathbb{R}^n$, as shown in Fig.1, we have

$$F_o = -J(x_o)F_e \tag{11}$$

where $J(x_o) = diag(J_i(x_o)) \in \mathbb{R}^{\bar{n}\times n}$, $F_e = [F_1^T, \cdots, F_m^T]^T$, here we denote $\bar{n} = \sum_1^m n_i$.

From equation (3), the dynamics of m manipulators can be written in a compact form

$$M(q)\ddot{x} + C(q,\dot{q})\dot{x} + G(q) = \tau_e + F_e \tag{12}$$

Since $\ddot{x}_i = \dot{J}_i(x_o)\dot{x}_o + J_i(x_o)\ddot{x}_o$, we can rewrite the dynamics of the ith manipulator in the following form:

$$\begin{aligned} &M(q)J(x_o)\ddot{x}_o + \big(M(q)\dot{J}(x_o) + C(q,\dot{q})\big)\dot{x}_o + G(q) \\ =&\tau_e + F_e \end{aligned} \tag{13}$$

where $q = [q_1^T, \cdots, q_m^T]^T \in \mathbb{R}^{\bar{N}}$, $J(x_o) = diag(J_i(x_o)) \in \mathbb{R}^{\bar{n}\times N}$, $M(q) = diag(M_i(q_i)) \in \mathbb{R}^{\bar{n}\times\bar{n}}$, $C(q,\dot{q}) = diag(C_i(q_i,\dot{q}_i)) \in \mathbb{R}^{\bar{n}\times\bar{n}}$, $\tau_e = [\tau_1^T, \cdots, \tau_m^T]^T \in \mathbb{R}^{\bar{n}\times 1}$, and denote $\bar{N} = \sum_1^m N_i$.

By multiplying left side of the equation (13) by $J^T(x_o)$, integrating equation (10) and (11), we have

$$\mathcal{M}(q,x_o)\ddot{x}_o + \mathcal{C}(q,\dot{q},x_o,\dot{x}_o)\dot{x}_o + \mathcal{G}(q,x_o,\dot{x}_o) = \tau - F_d \tag{14}$$

where $\mathcal{M}(q,x_o) = J^T(x_o)M(q)J(x_o) + M_o \in \mathbb{R}^{n\times n}$, $\mathcal{C}(q,\dot{q},x_o,\dot{x}_o) = J^T(x_o)(M(q)\dot{J}(x_o) + C(q,\dot{q})J(x_o)) + C_o(x_o) \in \mathbb{R}^{n\times n}$, $\mathcal{G}(q,x_o,\dot{x}_o) = J^T(x_o)G(q) + G_o \in \mathbb{R}^{n\times 1}$, $\tau = J^T(x_o)\tau_e \in \mathbb{R}^{n\times 1}$.

B. Trajectory Generation

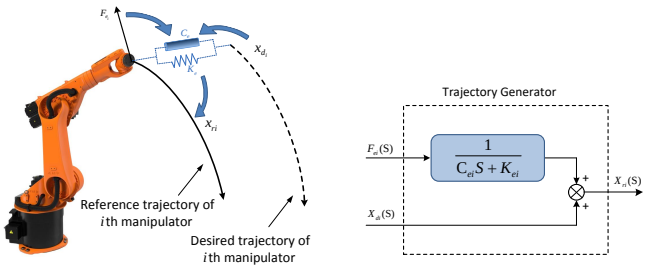

(a) (b)

Fig. 2. Admittance model. (a) the illustration of admittance model. (b) the flowchart of trajectory generator

In this paper, a damping-stiffness system model (Fig.2) is considered:

$$C_e\dot{x} + K_e x = F_e \tag{15}$$

where C_e and K_e are damping and stiffness parameters of the interaction system predefined by the experimenter, and F_e is the impedance force exerted on the end-effector. In general, a target admittance model in the Cartesian Space is depicted as below:

$$C_{e_i}(\dot{x}_{r_i} - \dot{x}_{d_i}) + K_{e_i}(x_{r_i} - x_{d_i}) = F_{e_i} \tag{16}$$

where x_{r_i} and x_{d_i} are reference trajectory and desired trajectory of the ith manipulator, respectively, as shown in Fig.2(a).

Applying Laplace transformation on (16), we can obtain:

$$C_{e_i}S\left[X_{r_i}(S) - X_{d_i}(S)\right] + K_{e_i}\left[X_{r_i}(S) - X_{d_i}(S)\right] = F_{e_i}(S) \tag{17}$$

and we can further obtain that

$$X_{r_i}(S) = \frac{F_{ei}(S)}{C_{ei}S + K_{ei}} + X_{di}(S) \tag{18}$$

Therefore, once the impedance force F_{e_i} and the desired trajectory x_{d_i} are obtained, the reference trajectory x_{r_i} could easily produced by the trajectory generator, the process can be seen in Fig.2(b).

Remark 1: As shown in Fig.2(b), the inputs of trajectory generator are force $F_{e_i}(S)$ and desired trajectory $X_{d_i}(S)$, the output is reference trajectory $X_{r_i}(S)$. Therefore, the generator can be regarded as a filter, which means the reference trajectory is obtained by filtering the impedance force and desired trajectory.

According to the task that multi-manipulators system need to perform, the desired trajectory of the object x_d in the Cartesian Space can be determined. Then the desired trajectory for each manipulator x_{d_i} could be specified by the experimenter in advance, which locates on the object and closer to the centre than the actual contact point between manipulator and the object does. It can be seen clearly in Fig.2(a), as the reference trajectory x_{r_i} and the desired trajectory x_{d_i} is different, the force between the manipulator and the object $F_{e_i} \neq 0$. Once the force obtained from pressure sensors mounted on the manipulators, the reference trajectory x_{r_i} can be derived by using admittance model. The relationship of desire object trajectory x_d, the desired manipulator trajectory x_{d_i} and the reference manipulator trajectory x_{r_i} can be seen in Fig.1.

Denoting $e_{rd_i} = x_{r_i} - x_{d_i}$, we have

$$\begin{aligned} \dot{e}_{rd_i} &= -\frac{K_{e_i}}{C_{e_i}}e_{rd_i} + \frac{1}{C_{e_i}}F_{e_i} \\ &\triangleq A_i e_{rd_i} + B_i F_{e_i} \end{aligned} \tag{19}$$

According to the knowledge of linear system, we can deduce that

$$e_{rd_i}(t) = e^{A_i t}x_{0_i} + \int_0^t e^{A_i(t-\tau)}B_i F_{e_i}(\tau)d\tau \tag{20}$$

where x_{0_i} is the initial state of the ith robot manipulator. Then we could get the reference trajectory:

$$\begin{aligned} x_{r_i}(t) &= e_{rd_i}(t) + x_{d_i} \\ &= e^{A_i t}x_{0_i} + \int_0^t e^{A_i(t-\tau)}B_i F_{e_i}(\tau)d\tau + x_{d_i} \end{aligned} \tag{21}$$

Assumption 3: The parameters of the ith admittance model is known, that means parameter matrix A_i and B_i also are known.

Assumption 4: The external forces exerted on the ith manipulator F_{e_i} can be measured by the pressure sensor mounted on the manipulator.

Remark 2: According to the assumption 3 and 4, considering the predetermined initial state x_{0_i} and desired trajectory x_{d_i}, we can conclude that the reference trajectory x_{r_i} could be generated by employing (21).

IV. CONTROL DESIGN

The objective of the NN control is to track the reference trajectory generated from section III-B. The framework of the multi-manipulator controller is shown in Fig.3.

Define the state variables $x_1 = x_o, x_2 = \dot{x}_o$, thus the kinetic equation in (14) can be rewritten as feedback form:

$$\begin{aligned} \dot{x}_1 &= x_2 \\ \dot{x}_2 &= \mathcal{M}^{-1}(x_1)\left(\tau - F_d - \mathcal{C}(x_1, x_2)x_2 - \mathcal{G}(x_1)\right) \end{aligned} \tag{22}$$

A. Controller Design using iBLF

The error variables are defined as follows

$$\begin{aligned} z_1 &= x_1 - x_d \\ z_2 &= x_2 - \alpha \end{aligned} \tag{23}$$

where error vector $z_1 = [z_{1i}, \cdots, z_{1n}]^T, z_2 = [z_{2i}, \cdots, z_{2n}]^T$, α represents virtual control aiming to let the tracking error z_1 converge to a small neighbourhood of zero.

Instead of using logarithmic Barrier Lyapunov Functions (BLF), a modified BLF method is employed in this paper, i.e. integral BLF, which allows the states constraints mixed with errors. For system (22), consider the iBLF candidate

$$V = \sum_{i=1}^{n} \int_0^{z_{1i}} \frac{\sigma k_{ci}^2}{k_{ci}^2 - (\sigma + \alpha_i)^2} d\sigma \tag{24}$$

where k_{ci} is positive constant satisfying $|x_i| < k_{ci}$. Then V is positive definite and continuously differentiable in the set $|\alpha_i| < k_{ci}$ for $i = 1, \cdots, n$. We denote the set $\mathcal{X} := \{x \in \mathbb{R}^n : |x_i| < k_{ci}, i = 1, \cdots, n\} \subset \mathbb{R}^n$.

Remark 3: The iBLF candidate V satisfies

$$\frac{z_i^2}{2} < V < z_i^2 \int_0^1 \frac{\beta k_{ci}^2}{k_{ci}^2 - (\beta z_i + \mathrm{sgn}(z_i) A_i)^2} d\beta \tag{25}$$

where $|x_{di}| \leqslant A_i < k_{ci}$, which is helpful for the proof of global stability. Additionally, a more useful conclusion can be given

$$\frac{z_i^2}{2} < V \leqslant \frac{k_{ci}^2 z_i^2}{k_{ci}^2 - x_{di}^2} \tag{26}$$

The proof of (26) can be seen in APPENDIX A.

We use backstepping method to design the controller. It consists of several steps.

Step 1 At the first step, we design the stabilizing function α_i. A positive Lyapunov Function is chosen as

$$V_1 = \sum_{i=1}^{n} \int_0^{z_{1i}} \frac{\sigma k_{ci}^2}{k_{ci}^2 - (\sigma + x_{di})^2} d\sigma \tag{27}$$

The time derivative of (27) is

$$\begin{aligned} \dot{V}_1 = &\sum_{i=1}^{n} \frac{k_{ci}^2 z_{1i}}{k_{ci}^2 - x_{1i}^2} (z_{2i} + \alpha_i - \dot{x}_{di}) \\ &+ \sum_{i=1}^{n} z_{1i} \left(\frac{k_{ci}^2}{k_{ci}^2 - x_{1i}^2} - \rho_i\right) \dot{x}_{di} \end{aligned} \tag{28}$$

where

$$\rho_i(z_{1i}, x_{di}) = \frac{k_{ci}}{2z_{1i}} \ln \frac{(k_{ci} + z_{1i} + x_{di})(k_{ci} - x_{di})}{(k_{ci} - z_{1i} - x_{di})(k_{ci} + x_{di})} \tag{29}$$

Using L'Hôpital's rule, it can be shown that

$$\begin{aligned} &\lim_{z_{1i} \to 0} \rho_i(z_{1i}, x_{di}) \\ =&\lim_{z_{1i} \to 0} \frac{k_{ci}}{2z_{1i}} \ln \frac{(k_{ci} + z_{1i} + x_{di})(k_{ci} - x_{di})}{(k_{ci} - z_{1i} - x_{di})(k_{ci} + x_{di})} \\ =&\frac{k_{ci}^2}{k_{ci}^2 - x_{di}^2} \end{aligned} \tag{30}$$

Since $|x_{di}| < k_{ci}$, $\rho_i(z_{1i}, x_{di})$ is well-defined in a neighbourhood of $z_{1i} = 0$ and singularity problem does not exist.

Then the virtual control $\alpha_i, i = 1, \cdots, n$ is designed as

$$\alpha_i = -\kappa_{1i} z_{1i} + \frac{(k_{ci}^2 - x_{1i}^2)\dot{x}_{di}\rho_i}{k_{ci}^2} \tag{31}$$

where κ_{1i} is a positive control gain and denote $K_1 = diag(\kappa_{11}, \cdots, \kappa_{1n})$. Substituting (31) into (28), we obtain

$$\dot{V}_1 = -\sum_{i=1}^{n} \frac{\kappa_{1i} k_{ci}^2 z_{1i}^2}{k_{ci}^2 - x_{1i}^2} + \sum_{i=1}^{n} \frac{k_{ci}^2 z_{1i} z_{2i}}{k_{ci}^2 - x_{1i}^2} \tag{32}$$

Step 2 A positive iBLF is chosen as

$$V_2 = V_1 + \frac{1}{2} z_2^T \mathcal{M} z_2 \tag{33}$$

Applying (14) and (23), the time derivative of (33) is

$$\begin{aligned} \dot{V}_2 = &-\sum_{i=1}^{n} \frac{\kappa_{1i} k_{ci}^2 z_{1i}^2}{k_{ci}^2 - x_{1i}^2} + \sum_{i=1}^{n} \frac{k_{ci}^2 z_{1i} z_{2i}}{k_{ci}^2 - x_{1i}^2} \\ &+ z_2^T \big(\tau - F_d - \mathcal{G}_i(x_1) - \mathcal{C}_i(x_1, \dot{x}_1)\alpha_i \\ &- \mathcal{M}_i(x_1)\dot{\alpha}_i\big) \end{aligned} \tag{34}$$

Design the control input $F_{o_i}^*$ as

$$F_o^* = -\begin{pmatrix} \frac{k_{c1}^2 z_{11}}{k_{c1}^2 - x_{11}^2} \\ \vdots \\ \frac{k_{cn}^2 z_{1n}}{k_{cn}^2 - x_{1n}^2} \end{pmatrix} - K_2 z_2 + F_d + \mathcal{G} + \mathcal{C}\alpha_i + \mathcal{M}\dot{\alpha} \tag{35}$$

where $K_2 = diag(k_{21}, k_{22}, k_{23})$ is a positive gain matrix.

Substituting (35) into (34), we obtain

$$\begin{aligned} \dot{V}_2 = &-\sum_{i=1}^{n} \frac{\kappa_{1i} k_{ci}^2 z_{1i}^2}{k_{ci}^2 - x_{1i}^2} - z_2^T K_2 z_2 \\ \leqslant &-\sum_{i=1}^{n} \int_0^{z_{1i}} \frac{\sigma k_{ci}^2}{k_{ci}^2 - (\sigma + x_{di})^2} d\sigma - z_2^T K_2 z_2 \\ \leqslant &-\rho V_2 \end{aligned} \tag{36}$$

where $\rho = \min\left\{\min_{1 \leqslant i \leqslant n}(k_i), \frac{2\lambda_{\min}(K_2)}{\lambda_{\max}(M)}\right\}$, with $\lambda_{\min}(\cdot)$, $\lambda_{\max}(\cdot)$ denoting the maximum and the minimum eigenvalue of $(\cdot)$, respectively. To ensure $\rho > 0$, parameters must satisfy $\min_{1 \leqslant i \leqslant n}(k_i) > 0$, $\frac{2\lambda_{\min}(K_2)}{\lambda_{\max}(M)} > 0$. Then V_2 will converge into a small neighbourhood near zero with the convergence rate of $e^{-\lambda}$.

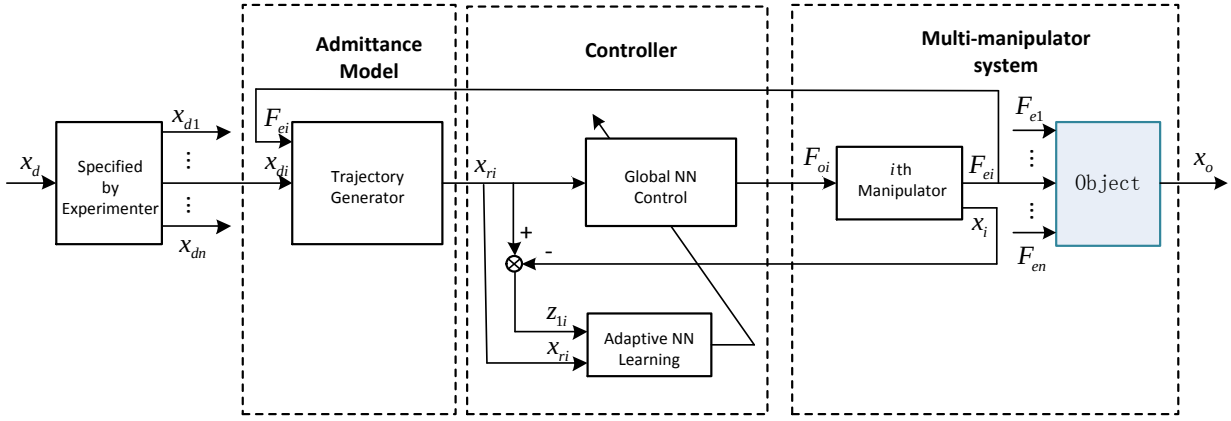

Fig. 3. The framework of the multi-manipulator controller

B. Global NN Control

In this paper, the switching functions $Q(Z) \in \mathbb{R}^{n\times n}$ are defined as follows:

$$Q(Z) = \text{diag}\left(M_1(Z), \cdots, M_n(Z)\right) \tag{37}$$

where $M_i(Z) = \prod_{k=1}^{\nu_i} m(z_k)$ with $Z = [x_1^T, x_2^T, \alpha^T, \dot{\alpha}^T]^T \in \mathbb{R}^{\nu_i}$, $\nu_i = 4n$, and $m(z_k)$ is given as

$$m(z_k) = \begin{cases} 1 & |z_k| < d_{1,k} \\ \frac{d_{2,k}^2 - z_k^2}{d_{2,k}^2 - d_{1,k}^2} e^{\left(\frac{z_k^2 - d_{1,k}^2}{\omega\left(d_{2,k}^2 - d_{1,k}^2\right)}\right)^2} & otherwise \\ 0 & |z_k| > d_{2,k} \end{cases} \tag{38}$$

with positive constants $0 < d_{1,k} < d_{2,k}$ and positive constant $\omega \geq 1$.

Noted that there are uncertainties in $\mathcal{G}(x_1)$, $\mathcal{C}(x_1, \dot{x}_1)$, $\mathcal{M}(x_1)$, and F_d therefore F_o^* cannot be obtained in a real system. RBFNN are used to approximate the uncertainties in terms $\mathcal{G}(x_1)$, $\mathcal{C}(x_1, \dot{x}_1)$, $\mathcal{M}(x_1)$, F_d. Define

$$F(Z) = \mathcal{G}(x_1) + \mathcal{C}(x_1, \dot{x}_1)\alpha + \mathcal{M}(x_1)\dot{\alpha} + F_d \tag{39}$$

where $F(Z) = [f_1(Z), \cdots, f_n(Z)]$, $Z = [x_1^T, x_2^T, \alpha^T, \dot{\alpha}^T]^T$ is RBF neural network input.

Assumption 5: The functions $f_i(Z), i = 1, \cdots, n$ are unknown and bounded, and there exits known nonnegative smooth functions $f_i^U(Z)$ satisfying

$$|f_i(Z)| < f_i^U(Z) \quad \forall Z \in \mathbb{R}^{\nu_i} \tag{40}$$

$\hat{f}_i(Z)$ is the approximation of $f_i(Z)$ given by

$$\hat{f}_i(Z) = \hat{W}_i^T S_i(Z) \tag{41}$$

where $\hat{W}_i$ is the actual weight vector; $S_i(\cdot)$ is the basis function introduced by (8), $\hat{W}_i^*$ is optimal weight vector, $\tilde{W}_i = \hat{W}_i - \hat{W}_i^*$ is error weight vector.

Then, the proposed adaptive neural network controller is designed as

$$\begin{aligned} F_o = &- \begin{pmatrix} \frac{k_{c1}^2 z_{11}}{k_{c1}^2 - x_{11}^2} \\ \vdots \\ \frac{k_{cn}^2 z_{1n}}{k_{cn}^2 - x_{1n}^2} \end{pmatrix} - K_2 z_2 + \Phi^a \\ &+ \left(1 - Q(Z)\right)\Phi^b + K_r \,\text{sgn}(z_2) \end{aligned} \tag{42}$$

where $K_r = \text{diag}(k_{r1}, \cdots, k_{rn}) > 0$, Φ^a and Φ^b are designed as

$$\Phi_i^a = \hat{f}_i(Z), \quad \Phi_i^b = f_i^U(Z)\Gamma_i\left(\frac{f_i^U(Z) z_i}{\varpi}\right) \tag{43}$$

with ϖ being a positive parameter, $F^U(Z) = \text{diag}[f_1^U(Z), \cdots, f_n^U(Z)]$, $\Gamma_i(\cdot) = \tanh(\cdot)$.

To improve the performance of the control system, the updating law is designed as

$$\dot{\hat{W}}_i = -\Theta_i\left(Q_i(Z) S_i(Z) z_{2i} + \sigma_i \hat{W}_i\right) \tag{44}$$

where Θ_i is positive symmetric matrix; σ_i is positive constant. $\hat{W}_i S_i(Z)$ is the estimated values of $\hat{W}_i^* S_i(Z)$.

$$\hat{W}_i^* S_i(Z) = f_i(Z) - \epsilon_i \tag{45}$$

where ϵ_i is approximating error satisfying $\|\epsilon_i\| \leqslant \bar{\epsilon}_i$, $\bar{\epsilon}_i$ is positive constant.

Remark 4: In the adaptive NN controller proposed in (42), the term $K_2 z_2$ providing the error feedback, NN approximation function Φ_i^a, robust item Φ_i^b and switching function $Q_i(Z)$ work together to ensure the global tracking performance. The scheme is shown in Fig.4. Ω_0 is the neural networks approximation within the admissible region. It is noted that the scale of smooth function $m(\cdot)$ is $|m(\cdot)| = 1$ in the compact set Ω_1 and $|m(\cdot)| = 0$ outside the set Ω_2. Therefore, in the compact set Ω_1 ($|x_1| \leqslant d_1$), term Φ_i^a works to approximate $\hat{f}_i(Z)$. Outside the set Ω_2 ($|x_1| \geqslant d_2$), robust term Φ_i^b works to pull the state x_1 back to Ω_2. When $d_1 < |x_1| < d_2$, term $\Phi_i^a + \left(1 - Q_i(Z)\right)\Phi_i^b$ will pull the state back to the compact set Ω_1.

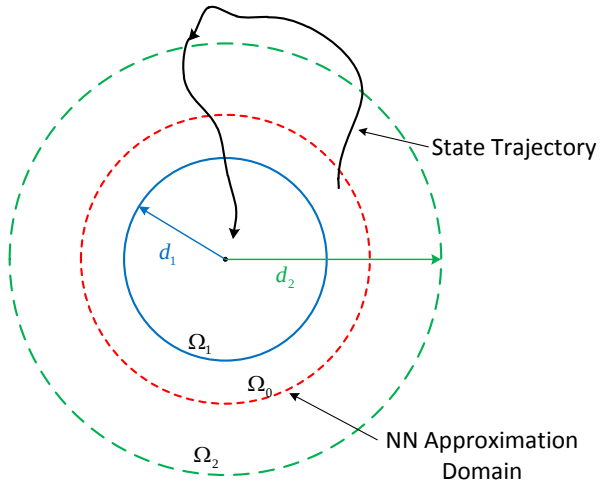

Fig. 4. The scheme of global control

C. Stability Analysis

Choose a positive iBLF as

$$V_3 = V_2 + \frac{1}{2}\sum_{i=1}^{n} \tilde{W}_i^T \Theta_i^{-1} \tilde{W}_i \tag{46}$$

Considering control input (42) and the derivative of (46), we have

$$\begin{aligned} \dot{V}_3 = &- \sum_{i=1}^{n} \frac{\kappa_{1i} k_{ci}^2 z_{1i}^2}{k_{ci}^2 - x_{1i}^2} - z_2^T K_2 z_2 + z_2^T \Big(\tilde{W}_i^T S_i(Z) \\ &- \epsilon_i + K_r \operatorname{sgn}(z_2) \Big) + \sum_{i=1}^{n} \tilde{W}_i^T \Theta_i^{-1} \dot{\hat{W}}_i \end{aligned} \tag{47}$$

Let us define ϵ_i as E_i, $i = 1, \cdots, n$ for the interval $t \in (0, +\infty)$, where $(\cdot)$ is ith element of a vector. Therefore, we obtain $E = [E_1, \cdots, E_n]^T$.

Substituting the weight updating laws into (47), we have

$$\begin{aligned} \dot{V}_3 = &- \sum_{i=1}^{n} \frac{\kappa_{1i} k_{ci}^2 z_{1i}^2}{k_{ci}^2 - x_{1i}^2} - z_2^T K_2 z_2 + z_2^T \left(K_r \operatorname{sgn}(z_2) - E \right) \\ &+ z_2^T \tilde{W}_i^T S_i(Z) - \sum_{i=1}^{n} \tilde{W}_i^T \left(S_i(Z) z_{2i} + \sigma_i \hat{W}_i \right) \end{aligned} \tag{48}$$

Notice that

$$z_2^T \tilde{W}_i^T S_i(Z) = \sum_{i=1}^{n} \tilde{W}_i^T S_i(Z) z_{2i} \tag{49}$$

and the gain matrix K_r are designed to satisfy $|E_i| \leqslant k_{ri}, i = 1, \cdots, n$, we have $z_2^T \left(K_r \operatorname{sgn}(z_2) - E \right) \leqslant 0$, therefore

$$\dot{V}_3 = - \sum_{i=1}^{n} \frac{\kappa_{1i} k_{ci}^2 z_{1i}^2}{k_{ci}^2 - x_{1i}^2} - z_2^T K_2 z_2 - \sum_{i=1}^{n} \tilde{W}_i^T S_i \hat{W}_i \tag{50}$$

Since $- \sum_{i=1}^{n} \tilde{W}_i^T S_i \hat{W}_i \leqslant \frac{\sigma_i}{2} \left(\sum_{i=1}^{n} W_i^{*T} W_i^* - \sum_{i=1}^{n} \tilde{W}_i^T \tilde{W}_i \right)$, we have

$$\begin{aligned} \dot{V}_3 \leqslant &- \sum_{i=1}^{n} \frac{\kappa_{1i} k_{ci}^2 z_{1i}^2}{k_{ci}^2 - x_{1i}^2} - z_2^T K_2 z_2 \\ &- \frac{\sigma_i}{2} \sum_{i=1}^{n} \tilde{W}_i^T \tilde{W}_i + \frac{\sigma_i}{2} \sum_{i=1}^{n} W_i^{*T} W_i^* \\ \leqslant &- \eta_3 V_3 + C_3 \end{aligned} \tag{51}$$

where $\eta_3 = \min \left\{ \kappa_{11}, \cdots, \kappa_{1n}, \frac{2\lambda_{\min}(K_2)}{\lambda_{\max}(\mathcal{M}_i)} > 0, \frac{\sigma_i}{\lambda_{\max}(\Theta_i^{-1})} > 0 \right\}$, $C_3 = \frac{\sigma_i}{2} \sum_{i=1}^{n} W_i^{*T} W_i^*$. To ensure $\eta_3 > 0$, $C_3 > 0$, controller parameters should possess some nature: $\kappa_{1i} > 0$, $\frac{2\lambda_{\min}(K_2)}{\lambda_{\max}(\mathcal{M}_i)} > 0$, $\frac{\sigma_i}{\lambda_{\max}(\Theta_i^{-1})} > 0$. Therefore, $\dot{V}_3$ is a negative definite function, and as time increases, V_3 will decay into a region close to zero.

Theorem 1: For the multiple manipulators system dynamics (14), under the NN controller (42) with weight updating law (44) and admittance trajectory generator (21), the system (14) would obtain satisfying control performance through environment-robot interaction force is imposed on (14). The errors will converge into a small neighbourhood near zero by designing appropriate controller parameters and updating laws. The system states still remain in the predefined region and the tracking error z_1 would converge into the compact $\Omega_{z_1} := \left\{ z_1 \in \mathbb{R}^n \,|\, |z_{1i}| \leqslant \sqrt{2B} \right\}$, $i = 1, \cdots, n$. The tracking error z_2 converge into the compact set $\Omega_{z_2} := \left\{ z_2 \in \mathbb{R}^n \,|\, |z_2| \leqslant \sqrt{\frac{2B}{\lambda_{max}(M)}} \right\}$, where $B := V_3(0) + \frac{C_3}{\eta_3}$. The proof of *Theorem 1* is given in APPENDIX B.

V. Simulation Studies

In this section, to illustrate the efficacy of the proposed adaptive control method, two sets of simulation studies are conducted and the results are compared, and the model of planar 2-link manipulators are employed in this paper as shown in Fig.5. The manipulators with force sensor on the end-effector cooperate to move an object along a predefined desired trajectory.

A. Robot Manipulator Model

Consider two homogeneous manipulators with 2 revolute joints [50]. These manipulators with force sensor mounted on the end-effectors share same parameters as listed in TABLE I, where m_i, l_i and $I_i, i = 1, 2$ are mass, length and inertia of the ith link, respectively.

TABLE I
Parameters of the manipulator

Parameters	Description	Values
m_{i1}	Mass of link 1	2.00 kg
m_{i2}	Mass of link 2	0.85 kg
l_{i1}	Length of link 1	0.30 m
l_{i2}	Length of link 2	0.30 m
I_{i1}	Inertia of link 1	0.045 kg·m^2
I_{i2}	Inertia of link 2	0.019 kg·m^2

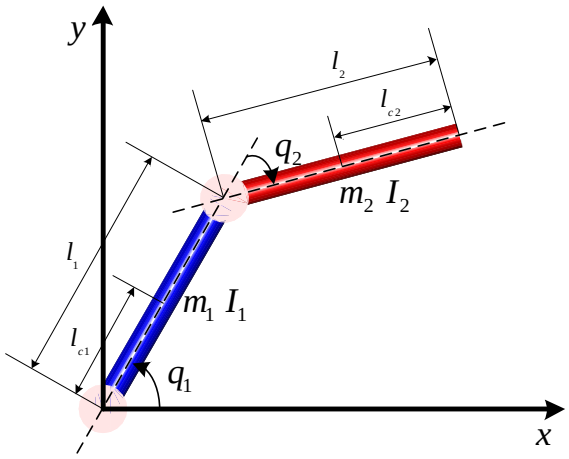

Fig. 5. The illustration of a planar 2-link manipulator

The carried object are chosen as a cube with its length $l_o = 0.1$m, mass $m_o = 0.1$kg and inertia $I_o = 0.1$kg·m^2. The desired trajectory of the mass centre of the object x_{do} is

$$x_{do} = \begin{bmatrix} x_{d1} \\ x_{d2} \\ \theta \end{bmatrix} = \begin{bmatrix} 0.2 * \cos(0.1t) \\ 0.2 * \sin(0.1t) \\ 0 \end{bmatrix}$$

which is a circle with the centre at $[0, 0]^T$ and radius being 0.1m and there is no rotation during the translation of the object. x_{d1} and x_{d2} are the x-coordinate and y-coordinate of the object, respectively, θ is the orientation of the object. The parameters of dynamics for the object are given as

$$M_o = \begin{bmatrix} 1 & 0 & 0 \\ 0 & 1 & 0 \\ 0 & 0 & 1 \end{bmatrix}, C_o = \begin{bmatrix} 1 & 0 & 0 \\ 0 & 1 & 0 \\ 0 & 0 & 1 \end{bmatrix}, G_o = \begin{bmatrix} 0 \\ -9.8 \\ 0 \end{bmatrix}.$$

Denote q_1, q_2 as the first and the second joint angles of the first manipulator, respectively. The position of the end-effector of the first manipulator in the Cartesian space are x_1 and x_2, respectively. Correspondingly, q_3, q_4, x_3 and x_4 are joint angles and position of the end-effector for the second manipulator. Therefore we have the following kinematic relationship

$$\begin{bmatrix} x_1 \\ x_2 \end{bmatrix} = \begin{bmatrix} l_1\ cosq_1 + l_2\ cos(q_1 + q_2) \\ l_1\ sinq_1 + l_2\ sin(q_1 + q_2) \end{bmatrix} + \begin{bmatrix} b_1 \\ 0 \end{bmatrix}$$

$$\begin{bmatrix} x_3 \\ x_4 \end{bmatrix} = \begin{bmatrix} l_1\ cosq_3 + l_2\ cos(q_3 + q_4) \\ l_1\ sinq_3 + l_2\ sin(q_3 + q_4) \end{bmatrix} + \begin{bmatrix} b_2 \\ 0 \end{bmatrix}$$

where $[b_1, 0]^T$ and $[b_2, 0]^T$ are the position of the bases of two manipulators. Therefore, the Jacobian matrix between the joint space of the manipulator and the corresponding Cartesian space is

$$J_{e,1}(q) = \begin{bmatrix} -l_1\ sinq_1 - l_2\ sin(q_1 + q_2) & -l_2\ sin(q_1 + q_2) \\ l_1\ cosq_1 + l_2\ cos(q_1 + q_2) & l_2\ cos(q_1 + q_2) \end{bmatrix}$$

$$J_{e,2}(q) = \begin{bmatrix} -l_1\ sinq_3 - l_2\ sin(q_3 + q_4) & -l_2\ sin(q_3 + q_4) \\ l_1\ cosq_3 + l_2\ cos(q_3 + q_4) & l_2\ cos(q_3 + q_4) \end{bmatrix}.$$

The Jacobian matrix between the end-effectors and the object J_o is

$$J_1(x_o) = \begin{bmatrix} 1 & 0 & \frac{l_o}{2} sin\theta \\ 0 & 1 & -\frac{l_o}{2} cos\theta \end{bmatrix}$$

$$J_2(x_o) = \begin{bmatrix} 1 & 0 & -\frac{l_o}{2} sin\theta \\ 0 & 1 & \frac{l_o}{2} cos\theta \end{bmatrix}$$

The dynamic parameters of the ith($i = 1, 2$) manipulator are

$$M_{e,i} = \begin{bmatrix} D_{i11} & D_{i12} \\ D_{i21} & D_{i22} \end{bmatrix}, C_{e,i} = \begin{bmatrix} C_{i11} & C_{i12} \\ C_{i21} & C_{i22} \end{bmatrix},$$
$$G_{e,i} = \begin{bmatrix} G_{i1}^T & G_{i2}^T \end{bmatrix}^T$$

where

$$\begin{aligned}
&D_{i11} = p_{i1} + 2p_{i2}cos(q_{i2}); && D_{i12} = p_{i3} + p_{i2}cos(q_{i2}); \\
&D_{i21} = p_{i3} + p_{i2}cos(q_{i2}); && D_{i22} = p_{i3}; \\
&C_{i11} = -p_{i2}sin(q_{i2})\dot{q}_{i2}; && C_{i12} = -p_{i2}sin(q_{i2})\dot{q}_{i2}; \\
&C_{i21} = p_{i2}sin(q_{i2})(\dot{q}_{i1} + \dot{q}_{i2}); && C_{i22} = 0; \\
&G_{i1} = (m_{i1}l_{c2} + m_{i2}l_{i1})gcos(q_{i1}) + m_{i2}l_{c2}gcos(q_{i1} + q_{i2}); \\
&G_{i2} = m_{i2}l_{c2}gcos(q_{i1} + q_{i2}); \\
&p_{i1} = m_{i1}l_{c1}^2 + m_{i2}(l_{i1}^2 + l_{c2}^2) + I_{i1} + I_{i2}; \\
&p_{i2} = m_{i2}l_{i1}l_{c2}; && p_{i3} = m_{i2}l_{c2}^2 + I_{i2};
\end{aligned}$$

where l_{c1} and l_{c2} are the centre of the first and the second link of the manipulator, respectively. Here q_{11}, q_{12}, q_{21} and q_{22} stand for q_1, q_2, q_3 and q_4, respectively.

B. Experimental Results

1) PD control: A conventional PD controller is designed as $\tau_{PD} = K_P z_1 + K_D z_2$, where the position error $z_1 = x_1 - x_d$ and velocity error $z_2 = \dot{z}_1 = x_2 - \dot{x}_d$, K_P and K_D are positive gain matrices. In this simulation study, the parameters are selected as $K_P = [5000, 5000, 1000]^T$ and $K_D = [450, 450, 350]^T$. The start position of the carried object is $[0.196, 0]$. The environmental disturbance is chosen as $F_d = [0.02 * sin(t), 0.02 * cos(t), 0]$. The total simulation duration is 90s and the sample time is 0.03s. Simulation results of PD control are shown in Fig. 6 - Fig. 10. Fig. 6 and 7 give the tracking performance of the PD controller and we can find that the tracking errors change with respect to time with a relative high vibration, as shown in Fig. 8 and 9. In Fig. 10, we can also find the control force is not stable and the amplitude is large.

2) Adaptive NN control:

For the neural network, the number of NN nodes are chosen as 2^{12}, the centre of NN nodes are evenly distributed in $[-1, 1]$, and the variance is 50. The NN weights are all initialized as zeros, the gain of NN adaptive law are chosen as $\Theta_1 = 120$, $\Theta_2 = 150$, $\Theta_3 = 120$, and $\sigma_1 = \sigma_2 = \sigma_3 = 0.001$. The designed parameters of the controller are selected as $K_1 = \text{diag}(15, 20, 15)$, $K_2 = \text{diag}(11, 15, 10)$ and $K_r = \text{diag}(0.01, 0.01, 0.01)$. The predefined bound of the position of the end-effector are $k_{c1} = k_{c2} = k_{c3} = 0.35$. The initial position of the mass centre of the object $x_o = [0.19, 0]^T$. The

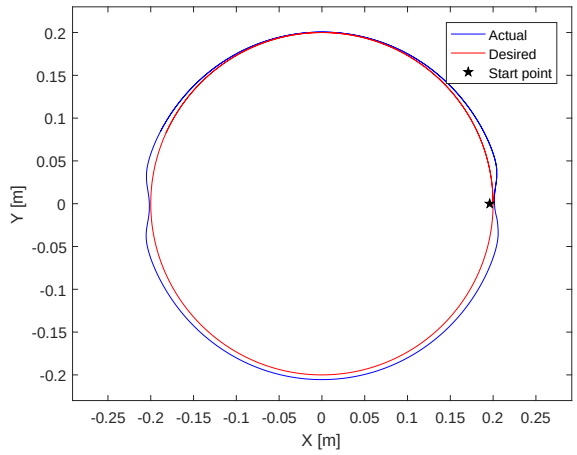

Fig. 6. Trajectory of the mass center of the object in XY plane (PD control)

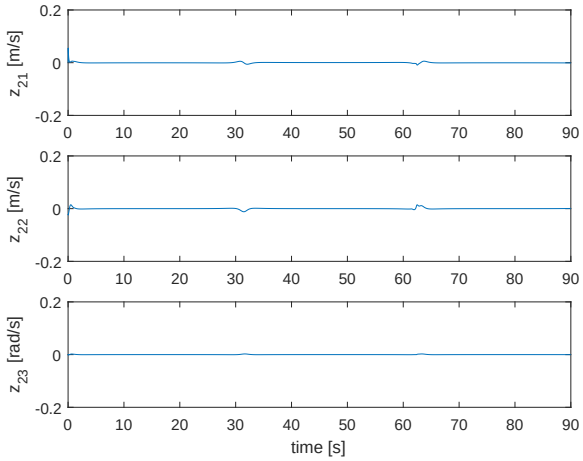

Fig. 9. Tracking error z_2 (PD control)

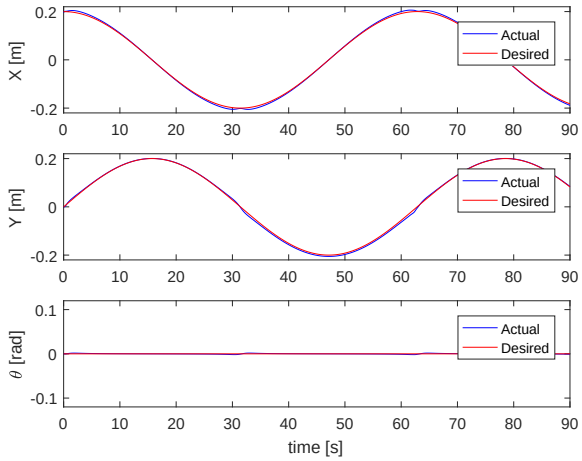

Fig. 7. Trajectories of the mass center of the object (PD control)

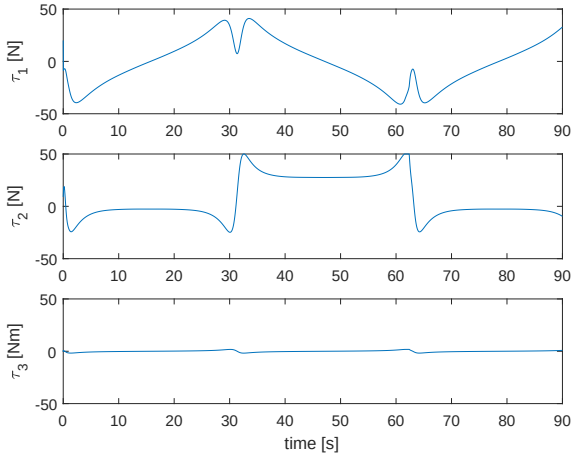

Fig. 10. The control torque exerted on the object (PD control)

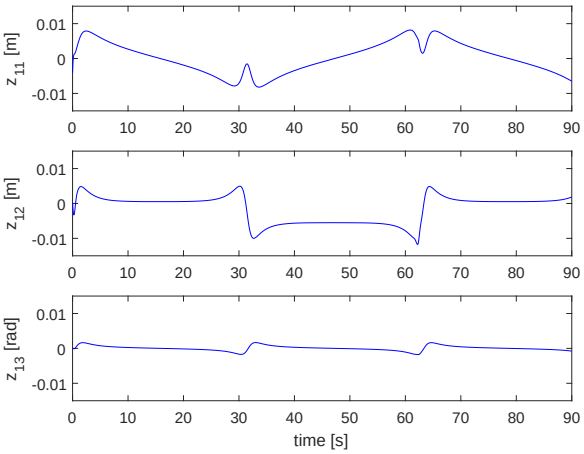

Fig. 8. Position tracking error of the object z_1 (PD control)

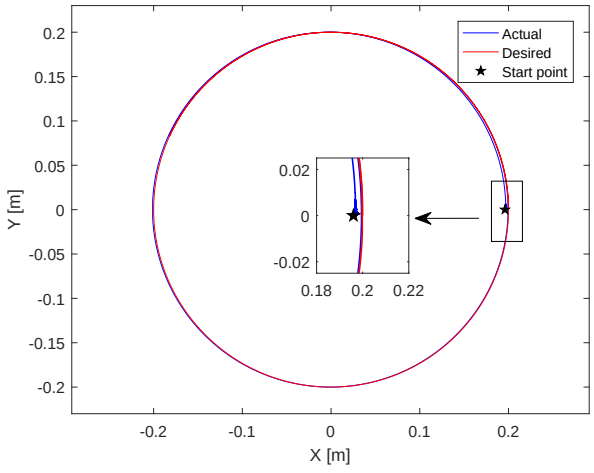

Fig. 11. Trajectory of the mass center of the object in XY plane (NN control)

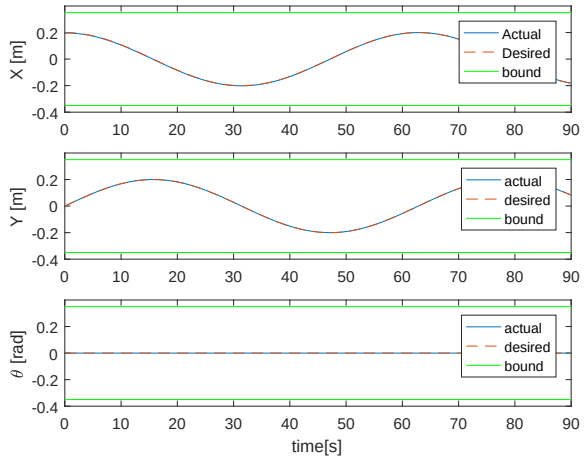

Fig. 12. Trajectories of the mass center of the object (NN control)

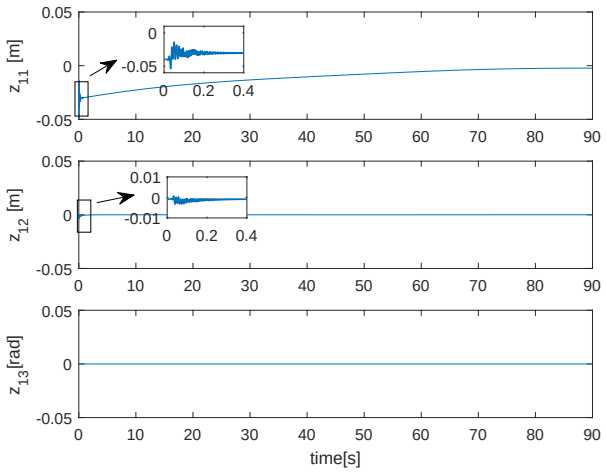

Fig. 13. Position tracking error of the object z_1 (NN control)

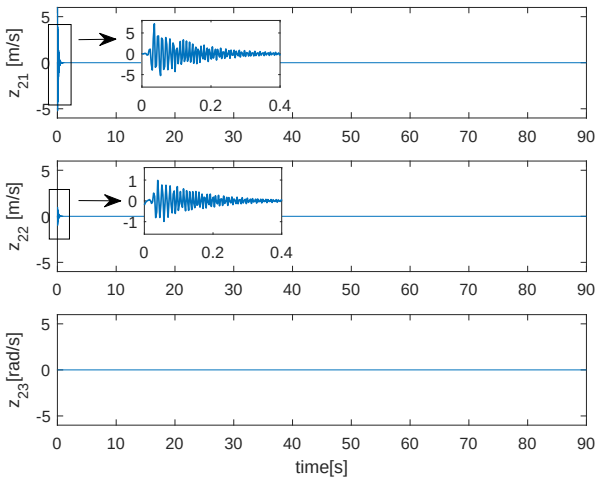

Fig. 14. Tracking error z_2 (NN control)

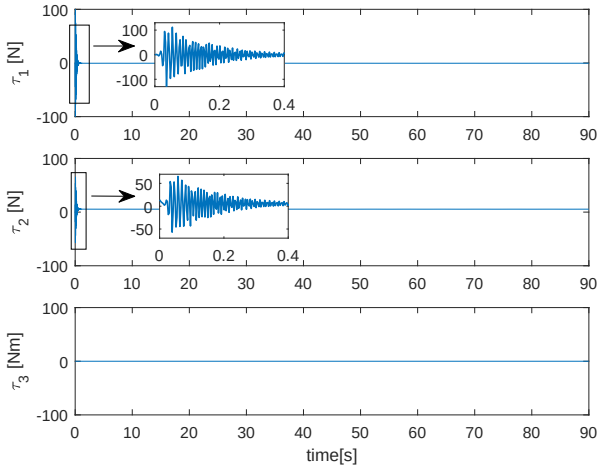

Fig. 15. The control torque exerted on the object (NN control)

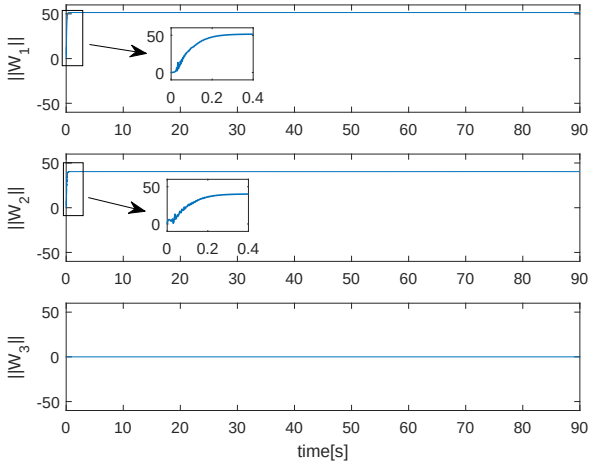

Fig. 16. Norms of the estimated NN weights (NN control)

disturbance and the simulation time are the same as the case for PD control.

The simulation results are shown in Fig. 11 - Fig. 16. Fig. 11 and 12 show the tracking trajectories of the NN control. In the proposed iBLF function based control method, positive constant k_{ci} stands for the output contraints. In our simulation, we set $k_{c1} = k_{c2} = k_{c3} = 0.35$. As shown in Fig. 12, the tracking trajectories remain in the predefined bound (green lines) during the whole simulation process, which validate the effectiveness of output constraints functionality of the proposed control scheme. From Fig. 13 and 14, the tracking errors converge to a small neighbourhood of zero quickly within 2 seconds, that is due to the learning process of the neural networks. In Fig.15, we can find that the control torque is stable at a relative low level when the NN weight matrix reach the optimal value. As depicted in Fig. 16, it takes less than 2 seconds for the estimated NN weight matrices to rapidly converge to stable values. In general, the NN control can make the controller more stable and efficient compared with PD control. These results verify the efficacy of the proposed method for the position tracking of the object carried by

multiple robot manipulators.

VI. Conclusion

This paper presents an adaptive control methodology based on admittance model for multiple manipulators transporting an rigid object cooperatively along a predefined desired trajectory. The admittance model is utilized to generate reference trajectory online for each manipulator according to the desired path of the rigid object. A type of iBLF is introduced to tackle the constraints due to the physical and environmental limits. As for the uncertainties of the manipulator dynamics, adaptive neural networks are employed to approximate these uncertain terms. The switching function provides the required the global stability of the closed-loop. The simulation results carried on planar 2-link manipulators validate the efficacy of the presented method. Although the performance of the adaptive NN control is better than that of the conventional PD control when the weight vector W is stable, it is noted that it takes a longer time for NN control to catch up with the desired signal. To further validate the proposed method, conducting some experiment is one of our future work.

Appendix

A. Proof of (26) in Remark 3

Step 1 (the left part of the inequality) Denote $g(z_i) = \int_0^{z_i} \frac{\sigma k_{ci}^2}{k_{ci}^2-(\sigma+\alpha_i)^2} d\sigma - \frac{z_i^2}{2} = \int_0^{z_i} \frac{\sigma(\sigma+\alpha_i)^2}{k_{ci}^2-(\sigma+\alpha_i)^2} d\sigma$, the derivative of $g(z_i)$ with regard to z_i is $\frac{\partial g}{\partial z_i} = \frac{z_i x_i^2}{k_{ci}^2-x_i^2}$. It is noted that in the compact set $\mathcal{X}$ we have $k_{ci}^2 - x_i^2 > 0$.

For case $z_i > 0$, we have $\frac{\partial g}{\partial z_i} < 0$; For case $z_i < 0$, we have $\frac{\partial g}{\partial z_i} > 0$. Since $g(z_i) = 0$ at $z_i = 0$, therefore we can draw the conclusion that $g_i > 0$ in the set $\mathcal{X}$. That means $\int_0^{z_i} \frac{\sigma k_{ci}^2}{k_{ci}^2-(\sigma+\alpha_i)^2} d\sigma > \frac{z_i^2}{2}$ holds in the set $\mathcal{X}$.

Step 2 (the right part of the inequality) Define $p_i(\sigma, \alpha_i) = \frac{\sigma k_{ci}^2}{k_{ci}^2-(\sigma+\alpha_i)^2}$, we have

$$\frac{\partial p_i}{\partial \sigma} = \frac{k_{ci}^2(k_{ci}^2 + \sigma^2 - \alpha_i^2)}{(k_{ci}^2 - x_i^2)^2} \tag{52}$$

which is positive in the set $|\sigma + \alpha_i| < k_{ci}$. Since $p_i(0, \alpha_{i-1}) = 0$ for all $|\alpha_i| < k_{ci}$ and $p_i(\sigma, \alpha_{i-1})$ is monotonically increasing with σ in the set $|\sigma + \alpha_i| < k_{ci}$, we further have $\int_0^{z_i} p_i(\sigma, \alpha_{i-1}) d\sigma \leqslant z_i p_i(\sigma, \alpha_{i-1})$ for $|\sigma + \alpha_i| < k_{ci}$, which leads to the right part of (26) after substituting for p_i.

B. Proof of Theorem 1

Multiplying $e^{\eta_3 t}$ on both sides of $\dot{V}_3 \leqslant -\eta_3 V_3 + C_3$, i.e. $(\dot{V}_3 + \eta_3 V_3)e^{\eta_3 t} \leqslant C_3 e^{\eta_3 t}$. After integration, there exists $V_3(t) \leqslant \left(V_3(0) - \frac{C_3}{\eta_2}\right) e^{-\eta_2 t} + \frac{C_3}{\eta_2} \leqslant V_3(0) + \frac{C_3}{\eta_2}$. Considering *Remark 3*, we know that $\frac{z_{1i}^2}{2} \leqslant \sum_{i=1}^{n} \frac{z_{1i}^2}{2} \int_0^{z_{1i}} \frac{\sigma k_{ci}^2}{k_{ci}^2-(\sigma+\alpha_i)^2} d\sigma \leqslant V_3(0) + \frac{C_3}{\eta_2}$. Further there are $|z_{1i}| \leqslant \sqrt{2B}$, $i = 1, \cdots, n$, $|z_2| \leqslant \sqrt{\frac{2B}{\lambda_{max}(M)}}$, where $B \coloneqq V_3(0) + \frac{C_3}{\eta_2}$.

References

[1] O. Lambercy, L. Dovat, R. Gassert, E. Burdet, C. L. Teo, and T. Milner, "A haptic knob for rehabilitation of hand function," *IEEE Transactions on Neural Systems and Rehabilitation Engineering*, vol. 15, no. 3, pp. 356–366, 2007.

[2] F. Chen, K. Sekiyama, F. Cannella, and T. Fukuda, "Optimal subtask allocation for human and robot collaboration within hybrid assembly system," *IEEE Transactions on Automation Science and Engineering*, vol. 11, no. 4, pp. 1065–1075, 2014.

[3] W. He, Z. Li, and C. L. P. Chen, "A survey of human-centered intelligent robots: issues and challenges," *IEEE/CAA Journal of Automatica Sinica*, vol. 4, no. 4, pp. 602–609, 2017.

[4] C. Sun, W. He, and J. Hong, "Neural network control of a flexible robotic manipulator using the lumped spring-mass model," *IEEE Transactions on Systems, Man, and Cybernetics: Systems*, vol. 47, no. 8, pp. 1863–1874, 2017.

[5] C. Yang, X. Wang, L. Cheng, and H. Ma, "Neural-learning-based telerobot control with guaranteed performance," *IEEE Transactions on Cybernetics*, 2016.

[6] W. He, Y. Chen, and Z. Yin, "Adaptive neural network control of an uncertain robot with full-state constraints," *IEEE Transactions on Cybernetics*, vol. 46, no. 3, pp. 620–629, 2016.

[7] Q. Guo, Y. Zhang, B. G. Celler, and S. W. Su, "Backstepping control of electro-hydraulic system based on extended-state-observer with plant dynamics largely unknown," *IEEE Transactions on Industrial Electronics*, vol. 63, no. 11, pp. 6909–6920, 2016.

[8] Q. Guo, J. Yin, T. Yu, and D. Jiang, "Saturated adaptive control of an electrohydraulic actuator with parametric uncertainty and load disturbance," *IEEE Transactions on Industrial Electronics*, vol. 64, no. 10, pp. 7930–7941, 2017.

[9] Y. Jin, P. H. Chang, M. Jin, and D. G. Gweon, "Stability guaranteed time-delay control of manipulators using nonlinear damping and terminal sliding mode," *IEEE Transactions on Industrial Electronics*, vol. 60, no. 8, pp. 3304–3317, 2013.

[10] C.-S. Chiu, K.-Y. Lian, and P. Liu, "Adaptive control of holonomic constrained systems: A feedforward fuzzy approximation-based approach," *IEEE transactions on control systems technology*, vol. 14, no. 3, pp. 456–466, 2006.

[11] Z. Li and C.-Y. Su, "Neural-adaptive control of single-master–multiple-slaves teleoperation for coordinated multiple mobile manipulators with time-varying communication delays and input uncertainties," *IEEE transactions on neural networks and learning systems*, vol. 24, no. 9, pp. 1400–1413, 2013.

[12] T. L. Huntsberger, A. Trebi-Ollennu, H. Aghazarian, P. S. Schenker, P. Pirjanian, and H. D. Nayar, "Distributed control of multi-robot systems engaged in tightly coupled tasks," *Autonomous Robots*, vol. 17, no. 1, pp. 79–92, 2004.

[13] Z. Li, C. Yang, C.-Y. Su, S. Deng, F. Sun, and W. Zhang, "Decentralized fuzzy control of multiple cooperating robotic manipulators with impedance interaction," *IEEE Transactions on Fuzzy Systems*, vol. 23, no. 4, pp. 1044–1056, 2015.

[14] Z. Li, W. Chen, and J. Luo, "Adaptive compliant force–motion control of coordinated non-holonomic mobile manipulators interacting with unknown non-rigid environments," *Neurocomputing*, vol. 71, no. 7, pp. 1330–1344, 2008.

[15] F. Aghili, "Adaptive control of manipulators forming closed kinematic chain with inaccurate kinematic model," *IEEE/ASME Transactions on Mechatronics*, vol. 18, no. 5, pp. 1544–1554, 2013.

[16] H. Bai and J. T. Wen, "Cooperative load transport: A formation-control perspective," *IEEE Transactions on Robotics*, vol. 26, no. 4, pp. 742–750, 2010.

[17] M. Honarpardaz, M. Tarkian, J. Ölvander, and X. Feng, "Finger design automation for industrial robot grippers: A review," *Robotics and Autonomous Systems*, vol. 87, pp. 104–119, 2017.

[18] F. Reuleaux and E. S. Ferguson, *Kinematics of machinery: outlines of a theory of machines*. Courier Corporation, 2012.

[19] I. Lenz, H. Lee, and A. Saxena, "Deep learning for detecting robotic grasps," *The International Journal of Robotics Research*, vol. 34, no. 4-5, pp. 705–724, 2015.

[20] S. Krut, V. Bégoc, E. Dombre, and F. Pierrot, "Extension of the form-closure property to underactuated hands," *IEEE Transactions on Robotics*, vol. 26, no. 5, pp. 853–866, 2010.

[21] A. Bicchi, "On the closure properties of robotic grasping," *The International Journal of Robotics Research*, vol. 14, no. 4, pp. 319–334, 1995.

[22] S. Part, "Impedance control: An approach to manipulation," *Journal of dynamic systems, measurement, and control*, vol. 107, p. 17, 1985.

[23] Z. Li, Z. Huang, W. He, and C.-Y. Su, "Adaptive impedance control for an upper limb robotic exoskeleton using biological signals," *IEEE Transactions on Industrial Electronics*, vol. 64, no. 2, pp. 1664–1674, 2017.

[24] M. Matinfar and K. Hashtrudi-Zaad, "Optimization-based robot compliance control: Geometric and linear quadratic approaches," *The International Journal of Robotics Research*, vol. 24, no. 8, pp. 645–656, 2005.

[25] M. T. Mason, "Compliance and force control for computer controlled manipulators," *IEEE Transactions on Systems, Man, and Cybernetics*, vol. 11, no. 6, pp. 418–432, 1981.

[26] W. He, T. Meng, X. He, and S. S. Ge, "Unified iterative learning control for flexible structures with input constraints," *Automatica*, vol. 96, pp. 326 – 336, 2018.

[27] X. Fu, S. Li, M. Fairbank, D. C. Wunsch, and E. Alonso, "Training recurrent neural networks with the levenberg–marquardt algorithm for optimal control of a grid-connected converter," *IEEE transactions on neural networks and learning systems*, vol. 26, no. 9, pp. 1900–1912, 2015.

[28] X. Fan, R. Y. Da Xu, L. Cao, and Y. Song, "Learning nonparametric relational models by conjugately incorporating node information in a network," *IEEE transactions on cybernetics*, vol. 47, no. 3, pp. 589–599, 2017.

[29] R.-H. Zhang, Z.-C. He, H.-W. Wang, F. You, and K.-N. Li, "Study on self-tuning tyre friction control for developing main-servo loop integrated chassis control system," *IEEE Access*, vol. 5, pp. 6649–6660, 2017.

[30] C. Sun and Y. Xia, "An analysis of a neural dynamical approach to solving optimization problems," *IEEE Transactions on Automatic Control*, vol. 54, no. 8, pp. 1972–1977, 2009.

[31] J. Li, C. Deng, R. Y. Da Xu, D. Tao, and B. Zhao, "Robust object tracking with discrete graph-based multiple experts," *IEEE Transactions on Image Processing*, vol. 26, no. 6, pp. 2736–2750, 2017.

[32] Y. Li, R. Cui, Z. Li, and D. Xu, "Neural network approximation-based near-optimal motion planning with kinodynamic constraints using rrt," *IEEE Transactions on Industrial Electronics*, 2018.

[33] C. Yang, Y. Jiang, Z. Li, W. He, and C.-Y. Su, "Neural control of bimanual robots with guaranteed global stability and motion precision," *IEEE Transactions on Industrial Informatics*, 2016.

[34] R. Yang, C. Yang, M. Chen, and A. S. Annamalai, "Discrete-time optimal adaptive rbfnn control for robot manipulators with uncertain dynamics," *Neurocomputing*, vol. 234, pp. 107–115, 2017.

[35] S. Jagannathan and F. L. Lewis, "Multilayer discrete-time neural-net controller with guaranteed performance," *IEEE Transactions on Neural Networks*, vol. 7, no. 1, pp. 107–130, 1996.

[36] C. Mu, Z. Ni, C. Sun, and H. He, "Air-breathing hypersonic vehicle tracking control based on adaptive dynamic programming," *IEEE transactions on neural networks and learning systems*, vol. 28, no. 3, pp. 584–598, 2017.

[37] G. K. Venayagamoorthy, R. G. Harley, and D. C. Wunsch, "Implementation of adaptive critic-based neurocontrollers for turbogenerators in a multimachine power system," *IEEE Transactions on Neural Networks*, vol. 14, no. 5, pp. 1047–1064, 2003.

[38] Y. Yang, D. Wunsch, and Y. Yin, "Hamiltonian-driven adaptive dynamic programming for continuous nonlinear dynamical systems," *IEEE transactions on neural networks and learning systems*, vol. 28, no. 8, pp. 1929–1940, 2017.

[39] Y. Pan, T. Sun, and H. Yu, "Peaking-free output-feedback adaptive neural control under a nonseparation principle," *IEEE transactions on neural networks and learning systems*, vol. 26, no. 12, pp. 3097–3108, 2015.

[40] J.-T. Huang, "Global tracking control of strict-feedback systems using neural networks," *IEEE transactions on neural networks and learning systems*, vol. 23, no. 11, pp. 1714–1725, 2012.

[41] B. Xu, C. Yang, and Y. Pan, "Global neural dynamic surface tracking control of strict-feedback systems with application to hypersonic flight vehicle," *IEEE Transactions on Neural Networks and Learning Systems*, vol. 26, no. 10, pp. 2563–2575, 2015.

[42] Y.-J. Liu, J. Li, S. Tong, and C. P. Chen, "Neural network control-based adaptive learning design for nonlinear systems with full-state constraints," *IEEE transactions on neural networks and learning systems*, vol. 27, no. 7, pp. 1562–1571, 2016.

[43] W. He, Z. Yin, and C. Sun, "Adaptive neural network control of a marine vessel with constraints using the asymmetric barrier lyapunov function," *IEEE transactions on cybernetics*, vol. 47, no. 7, pp. 1641–1651, 2017.

[44] S. Zhang, Y. Dong, Y. Ouyang, Z. Yin, and K. Peng, "Adaptive neural control for robotic manipulators with output constraints and uncertainties," *IEEE Transactions on Neural Networks and Learning Systems*, 2018.

[45] Y.-J. Liu and S. Tong, "Barrier lyapunov functions for nussbaum gain adaptive control of full state constrained nonlinear systems," *Automatica*, vol. 76, pp. 143–152, 2017.

[46] Z. Li, Z. Chen, J. Fu, and C. Sun, "Direct adaptive controller for uncertain mimo dynamic systems with time-varying delay and dead-zone inputs," *Automatica*, vol. 63, pp. 287–291, 2016.

[47] B. Siciliano and O. Khatib, *Springer handbook of robotics*. Springer, 2016.

[48] M. H. Stone, "The generalized weierstrass approximation theorem," *Mathematics Magazine*, vol. 21, no. 5, pp. 237–254, 1948.

[49] F. L. Lewis and D. Vrabie, "Reinforcement learning and adaptive dynamic programming for feedback control," *IEEE circuits and systems magazine*, vol. 9, no. 3, 2009.

[50] Y. Li, L. Chen, K. P. Tee, and Q. Li, "Reinforcement learning control for coordinated manipulation of multi-robots," *Neurocomputing*, vol. 170, pp. 168–175, 2015.

Yong Li received the B.Eng. degree in automatic control from Northwestern Polytechnical University, Xi'an, China, in 2013. He is currently pursuing the Ph.D. degree in the School of Marine Science and Technology, Northwestern Polytechnical University. His current research interests include adaptive control of multiple robots and control of marine vehicles.

Chenguang Yang (M'10-SM'16) is a Professor of Robotics. He received the Ph.D. degree in control engineering from the National University of Singapore, Singapore, in 2010 and performed postdoctoral research in human robotics at Imperial College London, London, UK from 2009 to 2010.

He has been awarded EU Marie Curie International Incoming Fellowship, UK EPSRC UKRI Innovation Fellowship, and the Best Paper Award of the IEEE Transactions on Robotics as well as over ten conference Best Paper Awards. His research interest lies in human robot interaction and intelligent system design.

Weisheng Yan received the B.Eng. degree in automatic control and Ph.D. degree in navigation, guidance and control from Northwestern Polytechnical University, Xi'an, China, in 1991 and 1999, respectively.

He is currently a Professor with the School of Marine Science and Technology, Northwestern Polytechnical University. His current research interests include guidance, navigation, and control of underwater vehicles.

Rongxin Cui (M'09) received the B.Eng. degree in autonomic control and the Ph.D. degree in control science and engineering from Northwestern Polytechnical University, Xi'an, China, in 2003 and 2008, respectively.,From August 2008 to August 2010, he was a Research Fellow with the Centre for Offshore Research and Engineering, National University of Singapore, Singapore.

He is currently a Professor with the School of Marine Science and Technology, Northwestern Polytechnical University, Xi'an, China. His current research interests include control of nonlinear systems, cooperative path planning and control for multiple robots, control and navigation for underwater vehicles, and system development.

Andy Annamalai received his M. Res in Communications Engineering and Digital signal processing from University of Plymouth in 2005 and a PhD in USV autopilot design from University of Plymouth in 2014.

He is currently a Senior Lecturer in the department of digital futures at the University of Winchester, Hampshire, England, UK. Prior to this tenure he was a Lecturer at the University of Highlands and Islands (UHI), Scotland, UK. He was a Member of the academic titles review board at UHI and actively contributed to the learning and teaching quality committee. This was preceded by his role as a Researcher at the Marine and Industrial Dynamic Analysis Research Group, Plymouth University, Devon, United Kingdom. He won the best paper award at the 25th IET Signals & Systems Conference 2014, Limerick, Ireland. He won the National Aeronautics and Space Administration (NASA) innovative solutions competition for the UK Southwest region, 2013.